

# Structure and structure relaxation

T. Franosch, W. Götze, M. R. Mayr, and A.P. Singh

*Physik-Department, Technische Universität München, 85747 Garching, Germany*

(J. Non-Cryst. Solids, in print)

## Abstract

A discrete-dynamics model, which is specified solely in terms of the system's equilibrium structure, is defined for the density correlators of a simple fluid. This model yields results for the evolution of glassy dynamics which are identical with the ones obtained from the mode-coupling theory for ideal liquid-glass transitions. The decay of density fluctuations outside the transient regime is shown to be given by a superposition of Debye processes. The concept of structural relaxation is given a precise meaning. It is proven that the long-time part of the mode-coupling-theory solutions is structural relaxation, while the transient motion merely determines an overall time scale for the glassy dynamics.

PACS numbers: 64.70.Pf, 61.20.Lc

## I. INTRODUCTION

Glass-forming liquids exhibit a dynamics which appears anomalous in comparison to the one of conventional condensed matter. The characteristic time scale  $\tau$  for the motion can be several orders of magnitude larger than the natural time scale of, say, normal liquid dynamics. The scale  $\tau$  is extremely sensitive to changes of control parameters such as temperature  $T$  or density  $n$ ; for example, a change of  $T$  by 10 degrees may imply a change of  $\tau$  by a factor 100. Furthermore, decay of correlations or spectra are stretched over dynamical windows of time  $t$  or frequency  $\omega$ , respectively, of many decades in size [1]. The evolution of the anomalous dynamics upon cooling or compressing a liquid has first been studied comprehensively by Li *et al.* [2,3] for the mixed salt  $\text{Ca}_{0.4}\text{K}_{0.6}(\text{NO}_3)_{1.4}$  (CKN) and by van Meegen and Underwood for a hard-sphere colloid [4]. The former determined depolarized-light-scattering spectra for a four-decade frequency window and the latter measured photon-correlation curves for an eight-decade time window. In recent years the mode-coupling theory (MCT) for the glass transition has been developed [5]. It deals with a mathematically well-defined model for anomalous dynamics, which results from a bifurcation point; its novel features are due to the interplay of non-linearities with divergent retardation times. Results of this theory have been tested against experiments, for example in Refs. [2-4]. The outcome of these tests qualifies MCT as a candidate for a theory of the anomalous dynamics in glass-forming liquids.

The equilibrium structure of a classical system is determined by the ratio of interaction potentials and thermal energy via the Boltzmann factors. It is independent of the particle masses or other inertia parameters. It is the same for a conventional system, ruled by Newton's equations of motion, and for a colloid, whose time evolution is controlled by a Brownian dynamics. The simplest information on structure is provided by the structure factor  $S_q \propto \langle |\varrho_{\vec{q}}|^2 \rangle$ , where  $\varrho_{\vec{q}}$  are density fluctuations of wave vector  $\vec{q}$ ; here and in the following  $q = |\vec{q}|$  denotes the vector modulus, and  $\langle \rangle$  abbreviates canonical averaging. The indicated anomalous dynamics in glassy systems is not related to anomalies of the

equilibrium structure;  $S_q$  is a smooth function of  $n, T$  and  $q$  throughout the whole liquid regime. The simplest information on structure dynamics is provided by the density correlators  $\Phi_q(t) = \langle \varrho_{\vec{q}}(t)^* \varrho_{\vec{q}} \rangle / \langle |\varrho_{\vec{q}}|^2 \rangle$ . The evaluation of these functions is the main theme of MCT. In this paper we will restrict ourselves to simple liquids and to the idealized version of the MCT [5].

Two propositions shall be considered. First, the anomalous dynamics is solely determined by the equilibrium structure, i.e., by the potential landscape in the configuration space. Second, the anomalous dynamics can be described by a superposition of Debye-relaxation processes:

$$\Phi_q(t) = \sum_j \rho_{q,j} \exp(-\gamma_{q,j}t) , \quad \rho_{q,j} > 0 , \quad \gamma_{q,j} \geq 0 . \quad (1)$$

These propositions provide a precise meaning to the statement that the anomalous dynamics is structure relaxation.

Density correlators in conventional liquids exhibit the short-time expansion  $\Phi_q(t) = 1 - \frac{1}{2}(\Omega_q t)^2 + O(t^3)$ , where  $\Omega_q^2 = v^2 q^2 / S_q$ , with  $v^2 = (k_B T / m)$  denotes the bare phonon frequency [6]. This expansion contradicts Eq. (1). Furthermore, the thermal velocity  $v$  depends on the particle mass  $m$  and is therefore not an equilibrium quantity. It is necessary to formulate the propositions more precisely to avoid a conflict with the cited short-time behavior. Thereby some insight in the physics of glassy dynamics shall be provided.

## II. BASIC EQUATIONS

Within the Zwanzig-Mori formalism one can derive the equation

$$\partial_t^2 \Phi_q(t) + \Omega_q^2 \Phi_q(t) + \int_0^t M_q(t-t') \partial_{t'} \Phi_q(t') dt' = 0 , \quad (2)$$

where  $M_q(t)$  is a correlation function of fluctuating forces [6]. The kernel  $M_q(t)$  can be split into a regular part  $M_q^{\text{reg}}(t)$ , dealing with conventional liquid-state dynamics, and a contribution  $\Omega_q^2 m_q(t)$ , dealing with slowly fluctuating forces due to sluggishly moving struc-

ture:  $M_q(t) = M_q^{\text{reg}}(t) + \Omega_q^2 m_q(t)$ . Normal-state dynamics would then be obtained from the equation  $\mathcal{D}\Phi_q(t) = 0$ , where the abbreviation is used:

$$\mathcal{D}\Phi_q(t) = \partial_t^2 \Phi_q(t) + \Omega_q^2 \Phi_q(t) + \int_0^t M_q^{\text{reg}}(t-t') \partial_{t'} \Phi_q(t') dt' . \quad (3)$$

The subtleties of MCT are due to the approximation of  $m_q(t)$  as mode-coupling functional  $\mathcal{F}_q$ :

$$m_q(t) = \mathcal{F}_q(\Phi_k(t)) = \sum_{kp} V_{q,kp} \Phi_k(t) \Phi_p(t) . \quad (4)$$

Here the positive coefficients  $V_{q,kp}$  are given in terms of  $S_q$ , i.e. by the equilibrium structure.

The MCT equations of motion are

$$\mathcal{D}\Phi_q(t) + \Omega_q^2 \int_0^t m_q(t-t') \partial_{t'} \Phi_q(t') dt' = 0 . \quad (5)$$

The theory is specified by  $S_q$  and  $M_q^{\text{reg}}(t)$  where neither quantity reflects glass-dynamics anomalies. The Eqs. (3)–(5) are regular and  $\Omega_q^2, V_{q,kp}, M_q^{\text{reg}}(t)$  depend smoothly on control parameters. For mathematical convenience the wave-vector moduli are discretized to a set of  $M$  values up to some cutoff  $q_{\text{max}}$ . Thereby MCT deals with  $M$  nonlinear integro-differential equations of the Volterra type, which are coupled via the functional  $\mathcal{F}_q$ . A review of the derivation of the MCT equations, in particular of the explicit form of  $V_{q,kp}$ , and citations of the original papers can be found in Ref. [7].

Let us consider the hard-sphere system (HSS) as main example for the following demonstration of our results. Its equilibrium state is controlled by the packing fraction  $\varphi = \pi n d^3 / 6$ . As unit of length the particle diameter  $d$  is chosen. Wave vectors are considered up to the cutoff  $q_{\text{max}} = 40$  and we use  $M = 100$  equally spaced  $q$  values. The structure factor is evaluated within the Percus–Yevick theory [6]. Two models for the regular dynamics shall be studied. In the first one the regular kernel is dropped, so that

$$\mathcal{D}^{(1)}\Phi_q(t) = \partial_t^2 \Phi_q(t) + \Omega_q^2 \Phi_q(t) . \quad (6a)$$

This is a model with Newtonian dynamics where the transient deals with oscillations. The second model is obtained by dropping inertia effects and replacing the regular kernel by a

$q$ -independent friction term  $\nu$ . This is a model for a colloid where the transient deals with relaxators

$$\mathcal{D}^{(2)}\Phi_q(t) = \nu\partial_t\Phi_q(t) + \Omega_q^2\Phi_q(t) . \quad (6b)$$

Another set of examples shall be formulated for a so-called schematic model (SM), dealing with a single correlator  $\Phi(t)$  only [8]. The mode-coupling functional is specified as  $\mathcal{F}(\Phi(t)) = v_1\Phi(t) + v_2\Phi(t)^2$ , where  $v_1 \geq 0$ ,  $v_2 \geq 0$  denote coupling constants. Despite its apparent simplicity, this  $M = 1$  model reproduces some generic features of the MCT so faithfully, that it has been used as basis for a quantitative description of the evolution of anomalous dynamics of glycerol within the full gigahertz band [9]. For the regular motion we again consider the oscillator model, Eq. (6a), and the relaxator model, Eq. (6b). In addition we also study a soft-mode contribution to the regular dynamics. Here the transient, described by  $\mathcal{D} = \mathcal{D}^{(3)}$ , is given by a regular kernel in Eq. (3), which obeys the oscillator equation

$$(\partial_t^2 + \nu_0\partial_t + \Omega_0^2)M^{\text{reg}}(t) = 0 , \quad (7)$$

with initial conditions  $M^{\text{reg}}(0) = c_0$ ,  $\partial_t M^{\text{reg}}(0) = 0$ . Choosing a low soft-mode frequency  $\Omega_0$  we shall investigate the interference of slow regular dynamics with anomalous dynamics.

### III. ANOMALOUS MCT DYNAMICS

The solutions  $\Phi_q(t)$  of the MCT equations of motion decay to zero for large times as expected for a liquid, provided control parameters like  $n$  or  $1/T$  are smaller than some critical value  $n_c$  or  $1/T_c$ . However, for  $n \geq n_c$  or  $1/T \geq 1/T_c$  the solutions describe ideal glass states characterized by a positive Debye-Waller factor  $f_q = \Phi_q(t \rightarrow \infty)$  [5]. For the HSS one finds the bifurcation point for  $\varphi_c \approx 0.52$  [10], which is not too far from the experimental value 0.58 [4]. The evolution of the HSS dynamics for wave vector  $q = 10.6$ , calculated for the oscillation transient (6a), is shown in Fig. 1; and Figs. 2 and 3 exhibit the corresponding

fluctuation spectra  $\Phi_q''(\omega)$  and susceptibility spectra  $\chi_q''(\omega) = \omega\Phi_q''(\omega)$ , respectively. Here  $\Phi_q''(\omega) = \int_0^\infty \cos(\omega t)\Phi_q(t)dt$  is the Fourier cosine transform of the correlator. The wave vector  $q = 10.6$  is located close to the first minimum of the structure factor. For the SM the weak-coupling liquid regime is separated from the strong-coupling glass regime in the  $v_1 - v_2$ -plane by the parabola  $v_1^c = (2\lambda - 1)/\lambda^2$ ,  $v_2^c = 1/\lambda^2$ ,  $1/2 \leq \lambda < 1$  [8]. Figures 4–6 exhibit the evolution of the dynamics for the soft-mode model, Eq. (7), upon crossing the transition line at  $\lambda = 0.7$ . The Figs. 1–6 exhibit slow, control-parameter-sensitive, stretched dynamics. Obviously, the results for the HSS are similar to the corresponding ones for the SM and this exemplifies the relevance of the latter for a discussion of MCT findings. The shown anomalous dynamics can be understood from the asymptotic solutions of the MCT equations for long times and low frequencies near the transition, as explained in the preceding literature, e.g. in Ref. [11].

There is a qualitative difference for the short-time dynamics of the HSS between the results shown in Fig. 1 and the ones shown in Ref. [11] for the dynamics calculated for the relaxation transient, Eq. (6b). The correlators of the second model decrease monotonously while the correlators in Fig. 1 exhibit oscillations. These get more and more damped if  $\varphi$  increases towards  $\varphi_c$ . Increasing  $\varphi$  above  $\varphi_c$ , the oscillations become again rather pronounced in the glass state. These yield the oscillation bumps for the spectra  $\Phi_q''(\omega)$  for  $\omega > 10$  in Fig. 2, while the spectra for the colloid model decrease monotonously with increasing frequency [11]. Similar differences occur for the SM. The oscillations in Fig. 4 are different from the ones calculated in Ref. [12] for the transient (6a); and the correlators for the relaxation transient, Eq. (6b), do not show oscillations at all [7]. The fluctuation spectra in Fig. 5 exhibit two oscillation bumps for  $\omega > 0.1$ , the spectra calculated with Eq. (6a) have one bump for the glass states [12], and the ones for the relaxation transient (6b) have no bumps at all [7]. However, the long-time parts of the decay curves referring to the same mode-coupling functional  $\mathcal{F}_q$  coincide for the various models for the transient. This holds provided an appropriate overall shift of the curves parallel to the logarithmic abscissa is done in the figures. The statement is demonstrated in Figs. 7, 8 for the two HSS models and in Figs.

9, 10 for the three mentioned SMs.

The findings in Figs. 7–10 suggest the following precise formulation of the first proposition. The transient dynamics determines a time scale  $t_0$  so that for  $t \gg t_0$  the correlators can be written as

$$\Phi_q(t) = F_q(t/t_0) . \quad (8)$$

Here  $F_q$  is independent of the transient as quantified in Eq. (3) by  $\Omega_q$  and  $M_q^{\text{reg}}(t)$ . The long-time decay, its sensitive dependence on control parameters and also its dependence on  $q$ , is given by the master functions  $F_q$ , which are determined by the mode-coupling functional  $\mathcal{F}_q$ . Of course, the transient may also depend on control parameters, and this leads to a smooth variation of  $t_0$ . This effect results in the parallel shift of the  $n = 2$ ,  $\epsilon < 0$ -curves in Fig. 7 and similar offsets of the  $n = 1$ -curves in Figs. 9, 10. The proposition is meant as asymptotic result for the approach towards the critical point so that  $t_0$  is the limit result at the bifurcation singularity.

#### IV. THE REGULAR PART $t_0$ OF THE RELAXATION SCALES

The first step of the proof of the first proposition is based on the leading and next-to-leading long-time expansion of the critical correlators, i.e., of the MCT solutions at the bifurcation point:

$$\Phi_q(t) = f_q^c + h_q(t_0/t)^a \{1 + [K_q + \kappa(a)](t_0/t)^a\} . \quad (9)$$

Here terms of order  $(t_0/t)^{3a}$  have been dropped. There are straightforward formulas for the evaluation of the critical form factor  $f_q^c > 0$ , the critical amplitude  $h_q > 0$ , the correction amplitude  $[K_q + \kappa(a)]$ , and the critical exponent  $a$ ,  $0 < a < 0.5$ , from the mode-coupling functional [11]. These parameters are equilibrium quantities. For the HSS one gets  $a = 0.312$ ,  $f_{10.6}^c = 0.417$ ,  $h_{10.6} = 0.642$ ,  $K_{10.6} + \kappa(a) = -0.185$ . For the SM one finds  $a = 0.327$ ,  $f^c = 0.3$ ,  $h = 0.7$ ,  $K = 0$ ,  $\kappa(a) = 0.0528$ . The transient, no matter how complicated

$M_q^{\text{reg}}(t)$  in Eq. (3) may be, merely enters via the scale  $t_0$ . Specializing Eq. (8) to the critical point, one identifies  $t_0$  with the scale in the proposition. There are two diverging time scales hidden in  $\Phi_q(t)$ , which govern its sensitive control–parameter dependence [5]. Formula (8) implies, that  $t_0$  enters these scales as a prefactor. The singular part of the scales is determined by the master functions  $F_q(\tilde{t})$ .

The found results are demonstrated in Figs. 11 and 12. For all models of Sec. II, Eq. (9) was matched to the numerical solution at the critical point. This determines the values  $t_0$ , cited in the figure captions. Notice in Fig. 12 that a larger percentage of the decay of  $\Phi(t)$  is described by the law (9) for the relaxator model than for the oscillator models. Slow transient oscillations can destroy the short–time part of the critical fractal decay. Given an upper time cutoff  $t_{\text{max}}$ , the transient oscillations can be modeled so that they destroy the critical decay for  $t \leq t_{\text{max}}$  completely. However, the decay for  $t > t_{\text{max}}$  is robust. One can construct models so that there is a fully developed  $\alpha$  process, i.e., a stretched decay of  $\Phi_q(t)$  from  $f_q^c$  to zero, without a critical decay precursor.

## V. A DISCRETE–DYNAMICS MODEL

The second step of the proof of Eq. (8) is based on the Fourier–Laplace transform of the equations of motion (3), (5):  $\Phi_q(\omega) = -1/[\omega - \Omega_q^2/[\omega + M_q^{\text{reg}}(\omega) + \Omega_q^2 m_q(\omega)]]$ . Here we use the convention for the transform of some function  $G(t)$  to  $G(\omega)$ :  $G(\omega) = i \int_0^\infty \exp(izt)G(t)dt$ ,  $z = \omega + i0$ . At the transition point one derives from Eq. (9) a divergent small–frequency mode–coupling kernel  $m_q(\omega) = [-\mathcal{F}_q(f_k^c)/\omega] + \mathcal{O}(1/\omega^{1-a})$ . Because of continuity one concludes that in the asymptotic limit of small frequencies and small separations from the critical point, the regular function  $\omega + M_q^{\text{reg}}(\omega)$  can be neglected in comparison to  $\Omega_q^2 m_q(\omega)$ . Hence, in this limit the correlators obey  $m_q(\omega) - \Phi_q(\omega) = \omega m_q(\omega)\Phi_q(\omega)$  [5]. Let us assume that  $\Phi_q(t)$  can be continued as a function  $F_q(t)$  to small times so, that the formulated equation holds for all times and frequencies:  $[N_q(\omega) - F_q(\omega)]/\omega = N_q(\omega)F_q(\omega)$ ,  $N_q(t) = \mathcal{F}_q(F_k(t))$ . The details of the continuation are of no concern, since we are not interested



in the short-time transient. Backtransformation yields the set of  $M$  implicit functional equations for the  $M$  functions  $F_q(t)$ :

$$\int_0^t [N_q(t') - F_q(t')] dt' = \int_0^t N_q(t-t') F_q(t') dt' , \quad (10a)$$

$$N_q(t) = \mathcal{F}_q(F_k(t)) , \quad q = 1, \dots, M . \quad (10b)$$

Equations of a similar form have been studied before in some different context [13,14], and we shall adopt some of the tricks of the preceding work to deal with the present problem. Notice that Eqs. (10) cannot define a time scale, since they are scale invariant. With  $F_q(t)$  also  $F_q^x(t) = F_q(x \cdot t)$  is a solution for all  $x > 0$ ,  $q = 1, \dots, M$ .

The integrals in Eq. (10a) shall be written as Riemann sums formed on a time grid of equal step size  $\delta$ . The sums shall be determined by the values of the functions in the middle of the intervals

$$g_q^{(i)} = F_q((i + 1/2)\delta) , \quad i = 0, 1, \dots . \quad (11)$$

The sums can be regrouped so that Eqs. (10) read

$$g_q^{(m)} = \mathcal{I}_q(g_k^{(0)}, g_k^{(1)}, \dots, g_k^{(m)}) , \quad (12a)$$

where the functional  $\mathcal{I}_q$  is given by

$$\mathcal{I}_q = \left\{ (1 - g_q^{(0)}) \mathcal{F}_q(g_k^{(m)}) + \sum_{i=0}^{m-1} [\mathcal{F}_q(g_k^{(i)}) - g_k^{(i)}] - \sum_{i=1}^{m-1} \mathcal{F}_q(g_k^{(m-i)}) g_q^{(i)} \right\} / [1 + \mathcal{F}_q(g_k^{(0)})] . \quad (12b)$$

Formula (12a) can be considered as an implicit equation to determine  $g_q^{(m)}$  in terms of the  $g_k^{(i)}$  for  $i$  preceding  $m$ :

$$g_q^{(m)} = \mathcal{T}_q(g_k^{(0)}, g_k^{(1)}, \dots, g_k^{(m-1)}) . \quad (13)$$

The explicit solution for  $g_q^{(m)}$ , i.e., the construction of the functional  $\mathcal{T}_q$ , is done by the following procedure. One defines a sequence of approximands  $g_{q,\ell}^{(m)}$ ,  $\ell = 0, 1, \dots$ , so that  $\lim_{\ell \rightarrow \infty} g_{q,\ell}^{(m)} = g_q^{(m)}$ . Here  $g_{q,\ell+1}^{(m)} = \mathcal{I}_q(g_k^{(0)}, \dots, g_k^{(m-1)}, g_{k,\ell}^{(m)})$ , and the start is chosen as

$g_{k,0}^{(m)} = g_k^{(m-1)}$ . Notice that the scale invariance is reflected by the fact, that the step size  $\delta$  does not occur in Eqs. (12), (13).

The result (13) can be interpreted as an iterated mapping with memory or, because of Eq. (11), as the definition of a discrete dynamics with retardation. The  $M \cdot m$  numbers  $g_k^{(i)}, k = 1, \dots, M, i = 0, \dots, m - 1$  determine the  $M$  numbers  $g_q^{(m)}$ . A sequence of values  $g_q^{(i)}$  is created, once that the  $M$  initial values  $g_q^{(0)}$  are specified. The arbitrariness of the scale is hidden in the one of the choice of the initial condition.

By construction one expects that the sequence defines a solution of Eqs. (10). To show this explicitly one can read all equations backwards. As an approximand for the  $F_q(t)$ , step functions are defined by  $F_q^\delta(t) = g_q^{(i)}$  for  $i < t/\delta \leq (i + 1)$ . Obviously,  $\lim_{\delta \rightarrow 0} F_q^\delta(t) = F_q(t)$  solves Eqs. (10), and these functions agree with the master functions in Eq. (8) for  $t$  large compared to the time scale  $t_0$ . The limit  $\delta \rightarrow 0$  for  $t \geq t_0$  is trivially taken by using Eq. (11) only in the limit  $i \rightarrow \infty$ . In practice, a large  $i_0$  is chosen and the  $g_q^{(i)}$  for  $i < i_0$  are considered as transient of the discrete mapping. For the prescribed small step size  $\delta$ ,  $\delta i_0$  has to be smaller than the lower bound of the time window to be studied. The found results are then independent of the indicated details, up to an overall time scale  $t_0$ . To cope with the stretching of the dynamics over many decades, we applied a decimation procedure [14].

The discrete dynamics and thus the master functions  $F_q$  have been constructed in Eqs. (11), (12), (13) solely in terms of the mode-coupling functional  $\mathcal{F}_q$ . Hence the function  $F_q$  in Eq. (8) is a quantity defined by equilibrium distributions. This finishes the proof of the first proposition. Figures 13 and 14 exhibit the construction of the master functions  $F_q(t)$  for the HSS and the SM. The corresponding results are included as dotted lines in Figs. 7–12.

Some side remark shall be added. Equations (10), specialized to the functional at the critical point and complemented by the initial condition  $F_q(t = 0) = f_q^c$ , are equivalent to the equation for the MCT  $\alpha$ -relaxation master function [5]. The specified iterated mapping used with initial condition  $g_q^{(0)} = f_q^c - \delta^* h_q$ ,  $\delta^* > 0$ ,  $\delta^* \rightarrow 0$ , is a very simple and most

efficient algorithm for the evaluation of  $F_q(t)$ .

## VI. COMPLETE MONOTONICITY

Let us combine Eqs. (5), (6b) to the MCT equations of motion for  $M$  relaxators, specified by the decay times  $\tau_q = \nu/\Omega_q^2$

$$\tau_q \partial_t \Phi_q(t) + \Phi_q(t) + \int_0^t m_q(t-t') \partial_{t'} \Phi_q(t') dt' = 0. \quad (14)$$

Suppose that the kernels  $m_q(t)$  are given as a superposition of  $L$  Debye processes:  $m_q^{(*)}(t) = \sum_{j=1}^L \mu_q^j \exp(-\Gamma_q^j t)$ , where  $\mu_q^j > 0$  and the rates are labeled so that  $0 < \Gamma_q^1 < \Gamma_q^2 < \dots < \Gamma_q^L$ . The Fourier–Laplace transform  $m_q^{(*)}(\omega)$  is a meromorphic function with  $L$  simple poles at  $-i\Gamma_q^j$ . Substitution of this result in the Fourier–Laplace transform of Eq. (14) yields the solution  $\Phi_q^{(*)}(\omega)$  as meromorphic function. Elementary discussion brings out that  $\Phi_q^{(*)}(\omega)$  has exactly  $(L+1)$  poles which are located on the imaginary axis at, say,  $(-i\gamma_q^j)$ ; the poles of  $m_q^{(*)}(\omega)$  separate those of  $\Phi_q^{(*)}(\omega)$ , i.e.,  $\Gamma_q^{j+1} > \gamma_q^j > \Gamma_q^j$  for  $j = 1, \dots, L-1$ ,  $\gamma_q^L > \Gamma_q^L$ ,  $\Gamma_q^1 > \gamma_q^0 > 0$ . The residues  $\rho_q^j$  of the poles are positive. Hence the solution is a superposition of  $(L+1)$  Debye processes  $\Phi_q^{(*)}(t) = \sum_{j=0}^L \rho_q^j \exp(-\gamma_q^j t)$ .

Neglecting the kernel  $m_q(t)$ , the solutions of Eq. (14) are Debye processes  $\Phi_q^{(0)}(t) = \exp(-t/\tau_q)$ . The relaxators are coupled by the mode–coupling functional (4), which is a polynomial with positive coefficients  $V_{q,kp}$ . Hence  $\mathcal{F}_q(\Phi_k^{(0)}(t)) = m_q^{(1)}(t)$  is a sum of a finite number, say  $L$ , Debye functions. Substitution of this kernel into Eq. (14), leads to a solution  $\Phi_q^{(1)}(t)$ , which according to the preceding paragraph is a sum of  $(L+1)$  Debye contributions. This can be used to define a new sum of Debye processes  $m_q^{(2)}(t) = \mathcal{F}_q(\Phi_q^{(1)}(t))$ . Continuing one constructs a sequence of approximands  $m_q^{(n)}(t)$ ,  $\Phi_q^{(n)}(t)$ ,  $n = 0, 1, 2, \dots$  of the type formulated in Eq. (1). In Ref. [15] it was shown: the sequence  $\Phi_q^{(n)}(t)$  converges uniformly towards the unique solutions of Eq. (14) and this solution is completely monotone, i.e., it obeys  $(-\partial/\partial t)^\ell \Phi_q(t) > 0$ ,  $\ell = 0, 1, \dots$ .

According to Bernstein’s theorem [16], every completely monotone function can be represented as Stieltjes integral

$$\Phi_q(t) = \int_0^\infty \exp(-\gamma t) d\alpha_q(\gamma) , \quad (15)$$

where the measure  $\alpha_q(\gamma)$  is an increasing function of the rate  $\gamma$ . The theory of these integrals implies the following. For every finite interval of positive times  $t$ ,  $0 < t_1 \leq t \leq t_2 < \infty$  and every positive error margin  $\eta$ , one can find a set of numbers  $\rho_q^j > 0, \gamma_q^j \geq 0, j = 1, \dots, N$ , so that

$$|\Phi_q(t) - \sum_{j=1}^N \rho_q^j \exp(-\gamma_q^j t)| < \eta . \quad (16)$$

The solutions of Eq. (14) can be approximated arbitrarily well by a finite sum of Debye processes.

Because of Eq. (8) the solutions of any MCT model are given for  $t \gg t_0$  by the transient independent function  $F_q(t/t_0)$ . This holds in particular for the solution of Eq. (14). Choosing  $t_1$  larger than  $t_0$  one can replace  $\Phi_q(t)$  by  $F_q(t/t_0)$  in Eq. (16). Thereby one obtains the precise formulation of the second proposition and its proof.

## VII. CONCLUSIONS

The dynamics of a classical system deals with the orbits in phase space. Collision events and vibrations are the elementary bits building the motion on microscopic scales. In dense liquids there is the cage effect [17]: the system gets trapped in phase space pockets for long times. This implies a separation of a low-frequency contribution to the spectra from the normal-motion band. This contribution is the anomalous dynamics dealing with the motion from one pocket to the other. The first proposition leads to the following picture. The anomalous dynamics reflects the statistics of orbits in configuration space. After coarse graining of the time over intervals of microscopic size, the normal condensed-matter dynamics does not play a role anymore; it merely sets the scale  $t_0$  for the exploration of the potential landscape in the high-dimensional configuration space. It does not matter, for example, whether this exploration is done as prescribed by Newton's equations of motion or by Brownian dynamics. Consequently, the correlation functions for the coarse-grained

dynamics are governed, up to an overall time scale  $t_0$ , only by Boltzmann factors, i.e. by equilibrium distribution functions.

The statistics of orbits is studied in the theory of generalized Brownian motion [18]. From this theory one expects as generic results time fractals like the one formulated in Eq. (9). These fractals result from the mapping of the orbits on the time axis as achieved by correlation functions. They reflect nontrivial Hausdorff dimensionalities of sets defined for return-time and waiting-time distributions. MCT should be viewed as a mathematical model allowing an explicit evaluation of such orbit statistics via the master functions  $F_q$  in Eq. (8) or via the discrete-dynamics procedure of Sec. V.

Debye's relaxation law is the paradigm for a dynamics without memory. Conventionally, it is derived by assuming random forces with a white-noise spectrum [6,17]. The derived Eqs. (1), (16) formulate a similar picture for the anomalous dynamics in glass-forming systems. Memory effects are irrelevant for the coarse-grained orbits through the potential landscape. At the first glance this finding appears as a contradiction to MCT, which deals with a retarded fluctuating force via the integral term in the equation of motion (5). Indeed, it is this memory term, which renders the MCT bifurcation scenario so different from what one knows for bifurcations of conventional dynamical systems. The solution of the paradox was explained in the first paragraph of Sec. VI. A white-noise spectrum is sufficient to produce the Debye law, but it is not necessary. If the forces are superpositions of  $L$  Debye laws, their retarded influence leads to a response, which is also a superposition of Debye laws albeit of  $(L+1)$  terms. The MCT memory effects do not destroy the complete monotonicity, i.e., the possibility for a representation as superposition of Debye processes. But the memory effects lead necessarily to a distribution of the relaxation rates, i.e. to relaxation stretching.

Our result (8) implies that the susceptibility spectra can be written as  $\chi_q''(\omega) = \hat{\chi}_q(\omega t_0)$ . Here the master spectrum  $\hat{\chi}_q(\omega)$  is given by the equilibrium structure and it can be evaluated from the Fourier cosine transform  $F_q''(\omega)$  of the master functions  $F_q(t)$ , discussed in Sec. V:  $\hat{\chi}_q(\omega) = \omega F_q''(\omega)$ . This holds, provided the frequencies are sufficiently small compared to the characteristic scale  $1/t_0$ , which is determined by the transient. This conclusion is

demonstrated in Fig. 15 for the two HSS models. For  $n \geq 6$ , i.e. for  $|\epsilon| = |(\varphi - \varphi_c)/\varphi_c| \leq 10^{-2}$ , and  $\omega t_0 \leq 10^{-2.5}$  the spectra for the relaxator model (full lines) agree with those for the oscillator model (dashed lines), and both agree with the results obtained for the discrete-dynamics model (dotted lines). Two features of our findings should be emphasized. Firstly, the full lines represent spectra for the relaxator model, but only the part for  $\log_{10} \omega t_0 \leq -0.5$  is structural relaxation as given by  $\hat{\chi}_q(\omega t_0)$ . Due to mode-coupling effects there are non-Debye relaxation spectra, which deal with crossover phenomena from transient to structural-relaxation dynamics. The corresponding crossover window is much larger for the oscillator model; it extends over the window  $-2.5 < \log_{10} \omega t_0 < -0.5$ . Here the dashed curves in Fig. 15 can be described reasonably by an effective power law  $\chi_q''(\omega) = h_q^{\text{eff}}(\omega t_0)^{a_{\text{eff}}}$ , where the effective amplitude  $h_q^{\text{eff}}$  and the effective exponent  $a_{\text{eff}}$  depend on the control parameter  $\varphi$ . Secondly, the range of the applicability of Eq. (8) can be extended by incorporating the smooth control-parameter dependence of  $t_0$ , mentioned at the end of Sec. III. Thereby the  $\Phi(t)$  versus  $\log_{10}(t/t_0)$  diagrams, shown e.g. for  $\epsilon < 0$ ,  $n = 1$  in Fig. 9, get a shift parallel to the abscissa so that they coincide with the dotted line there. Similarly, negative shifts bring the low-frequency spectra in Fig. 15 for  $\epsilon < 0$ ,  $n = 4$  for the two HSS models on the master spectra, and positive shifts do the same for the  $\epsilon > 0$ ,  $n = 4$  results. The important point is, that the same shifts do the rescaling for all wave vectors  $q$  for the HSS.

The critical decay law (9) is the germ of all analytical results derived within MCT. It was first measured for CKN and that by inelastic neutron scattering [19], and by polarized as well as depolarized-light-scattering spectroscopy [20]. Later this part of the anomalous spectrum was also explored for a number of other systems like, for example, orthoterphenyl [21–23]. The function  $f + h/t^a$  with  $f > 0$ ,  $h > 0$  and  $0 < a < 1$  is completely monotone and thus it can be written as Eq. (1). The  $1/t^a$ -decay leads to a self-similar spectrum  $\Phi''(\omega) \propto \omega^{1-a}$ , which does not define a time scale. The time scales  $1/\gamma_q^j$  in Eq. (1) merely reflect the dynamical window, within which the critical law was studied. The representation of the critical spectrum by Debye peaks [22] is not an alternative, let alone a phenomenological theory, for the original formulation of the discovery [19–21], rather it is a reformulation in

a manner suggested by Bernstein's theorem. We have shown in Sec. VI that not only the critical spectrum, but the entire low-frequency spectrum can be represented as sum of Debye contributions.

#### **ACKNOWLEDGMENTS**

We thank H.Z. Cummins, M. Fuchs, and W. Kob for discussions and constructive criticism on our manuscript. Our work was supported by Verbundprojekt BMBF 03GO4TUM.

## REFERENCES

- [1] J. Wong and C. A. Angell, *Glass: Structure by Spectroscopy* (Marcel Dekker, Inc., New York, 1976).
- [2] G. Li *et al.*, Phys. Rev. A **45**, 3867 (1992).
- [3] H. Z. Cummins *et al.*, Phys. Rev. E **47**, 4223 (1993).
- [4] W. van Meegen and S. M. Underwood, Phys. Rev. E **49**, 4206 (1994).
- [5] W. Götze and L. Sjögren, Rep. Prog. Phys. **55**, 241 (1992).
- [6] J.-P. Hansen and I. R. McDonald, *Theory of Simple Liquids*, 2nd ed. (Academic Press, London, 1986).
- [7] W. Götze and L. Sjögren, Transp. Theory Stat. Phys. **24**, 801 (1995).
- [8] W. Götze, Z. Phys. B **56**, 139 (1984).
- [9] T. Franosch, W. Götze, M. R. Mayr, and A. P. Singh, Phys. Rev. E **55**, 3183 (1997).
- [10] U. Bengtzelius, W. Götze, and A. Sjölander, J. Phys. C **17**, 5915 (1984).
- [11] T. Franosch *et al.*, Phys. Rev. E **55**, 7153 (1997).
- [12] W. Götze and L. Sjögren, Chem. Phys. **212**, 47 (1996).
- [13] W. Götze, J. Phys.: Condens. Matter **2**, 8485 (1990).
- [14] W. Götze, J. Stat. Phys. **83**, 1183 (1996).
- [15] W. Götze and L. Sjögren, J. Math. Analysis and Appl. **195**, 230 (1995).
- [16] W. Feller, *Introduction to Probability Theory*, 2nd. ed. (Wiley, New York, 1971), Vol. II.
- [17] U. Balucani and M. Zoppi, *Dynamics of the Liquid State* (Clarendon Press, Oxford, 1994).



- [18] K. Ito and H. P. McKean, *Diffusion processes and their sample paths* (Springer, Berlin, 1965).
- [19] W. Knaak, F. Mezei, and B. Farago, *Europhys. Lett.* **7**, 529 (1988).
- [20] N. J. Tao, G. Li, and H. Z. Cummins, *Phys. Rev. Lett.* **66**, 1334 (1991).
- [21] W. Petry *et al.*, *Z. Phys. B* **83**, 175 (1991).
- [22] W. Steffen, A. Patkowski, G. Meier, and E. W. Fischer, *J. Chem. Phys.* **96**, 4171 (1992).
- [23] H. Z. Cummins *et al.*, *Prog. Theor. Phys.* **126**, 21 (1997).

## FIGURES

FIG. 1.

Density correlators for the HSS for wave vector  $q = 10.6$  calculated for the oscillator transient, Eq. (6a). The time unit is chosen so that  $v/d = 2.5$ . Curve  $c$  refers to the critical packing fraction  $\varphi = \varphi_c$ . The uppermost curve is calculated for  $\varphi = 0.60$ , and the other curves refer to  $(\varphi - \varphi_c)/\varphi_c = \epsilon = \pm 1/10^{n/3}$ ,  $n = 0, 1, \dots$ . The free-oscillator curve  $\Phi_q(t) = \cos \Omega_q t$ , which refers to  $\epsilon = -1$ , is drawn only for  $\Omega_q t \leq 1.98$ . The arrow marks the time  $t_0 = 0.00944$ .

FIG. 2.

Density fluctuation spectra for the results of Fig. 1.

FIG. 3.

Susceptibility spectra for the results of Fig. 1.

FIG. 4.

Correlators for the SM with soft-mode transient according to Eq. (7) with parameters  $\nu_0 = 0.2\Omega$ ,  $\Omega_0 = 0.5\Omega$ ,  $c_0 = 0.2$ . The time unit is chosen so, that  $\Omega = 1$ . Curve  $c$  refers to the critical point  $v_1^c = (2\lambda - 1)/\lambda^2$ ;  $v_2^c = 1/\lambda^2$ ,  $\lambda = 0.7$ . The others are calculated for  $v_{1,2} = v_{1,2}^c(1 + \epsilon)$ ,  $\epsilon = \pm 1/4^n$ ,  $n = 0, 1, \dots$ . The arrow marks the time  $t_0 = 0.0649$ .

FIG. 5.

Fluctuation spectra for the results of Fig. 4.

FIG. 6.

Susceptibility spectra for the results of Fig. 4.

FIG. 7.

Curves (1) are  $\epsilon < 0$  results from Fig. 1 replotted with scale  $t_0 = 0.00944$ . Curves (2) are the corresponding results for the relaxation transient, Eq. (6b), replotted from Ref. [11] with scale  $t_0 = 0.425$ . The dotted lines (3) are the discrete-dynamics-model results from Fig. 13, replotted with  $t_0 = 267\delta$ . The labels  $n$  are set as in Fig. 1. Curves for successive values of  $n$  are shifted horizontally by two decades in order to avoid overcrowding.

FIG. 8.

The analogous results as shown in Fig. 7 but for  $\epsilon > 0$ .

FIG. 9.

Curves (3) are  $\epsilon < 0$  results from Fig. 4 replotted with scale  $t_0\Omega = 0.0649$ . Curves (1) (and (2)) are the corresponding results calculated for the oscillation transient, Eq. (6a) (relaxation transient, Eq. (6b)) replotted from Ref. [12] (Ref. [7]) with scales  $t_0\Omega = 0.0440$  ( $t_0\nu = 0.150$ ). The dotted lines (4) are discrete-dynamics-model results from Fig. 14, replotted with scale  $t_0 = 26.2\delta$ . The labels  $n$  are set as in Fig. 4. Curves for successive values of  $n$  are shifted horizontally by two decades in order to avoid overcrowding.

FIG. 10.

The analogous results as shown in Fig. 9 but for  $\epsilon > 0$ .

FIG. 11.

Density correlators of the HSS for  $q = 10.6$  and the critical value  $\varphi_c$  for the packing fraction. Curve (1) is replotted from Fig. 1 with  $t_0 = 0.00944$ ; curve (2) refers to the relaxation transient, Eq. (6b), and it is replotted from Ref. [11] with  $t_0 = 0.425$ . Curve (3) refers to the discrete dynamics-model and is replotted from Fig. 13 with  $t_0 = 267\delta$ . Curve (5) exhibits the asymptotic expansion law, Eq. (9), and the curve (4) is the leading contribution to Eq. (9):  $\Phi_q(t) = f_q^c + h_q(t_0/t)^a$ .

FIG. 12.

Decay curves for the SM for the critical point  $\lambda = 0.7$ . Curve (1) refers to the oscillation model, Eq. (6a); it is taken from Ref. [12] and replotted with  $t_0\Omega = 0.0440$ . Curve (2) refers to the relaxation model, Eq. (6b); it is taken from Ref. [7] and replotted with  $t_0\nu = 0.1498$ . Curve (3) refers to the soft-mode model; it is replotted from Fig. 4 with  $t_0\Omega = 0.0649$ . Curve (4) refers to the discrete-dynamics model and it is replotted from Fig. 14 with  $t_0 = 26.2\delta$ . The dashed line (5) exhibits the asymptotic expansion law, Eq. (9).

FIG. 13.

Density correlators of the HSS for wave vector  $q = 10.6$  calculated for the discrete-dynamics model with initial condition  $g_q^{(0)} = 10$ . The time unit is chosen so that  $\delta = 1$  in Eq. (11). The labeling of the curves is done as in Fig. 1. The arrow marks the time  $t_0 = 267$ .

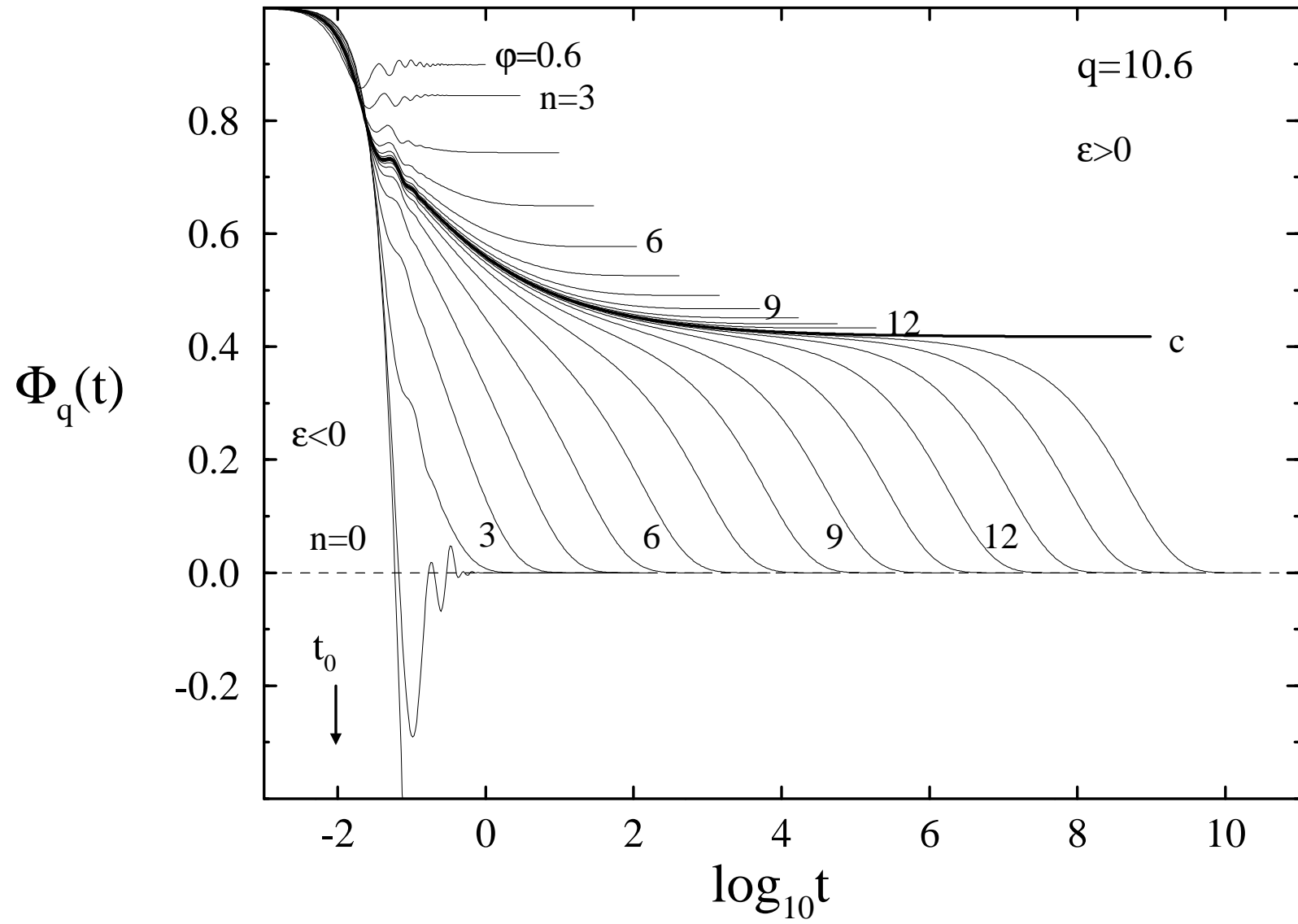
FIG. 14.

Correlators of the SM for the discrete dynamics with  $g^{(0)} = 10$ . The time unit is chosen so that  $\delta = 1$  in Eq. (11). The labeling of the curves is done as in Fig. 4. The arrow marks the time  $t_0 = 26.2$ .

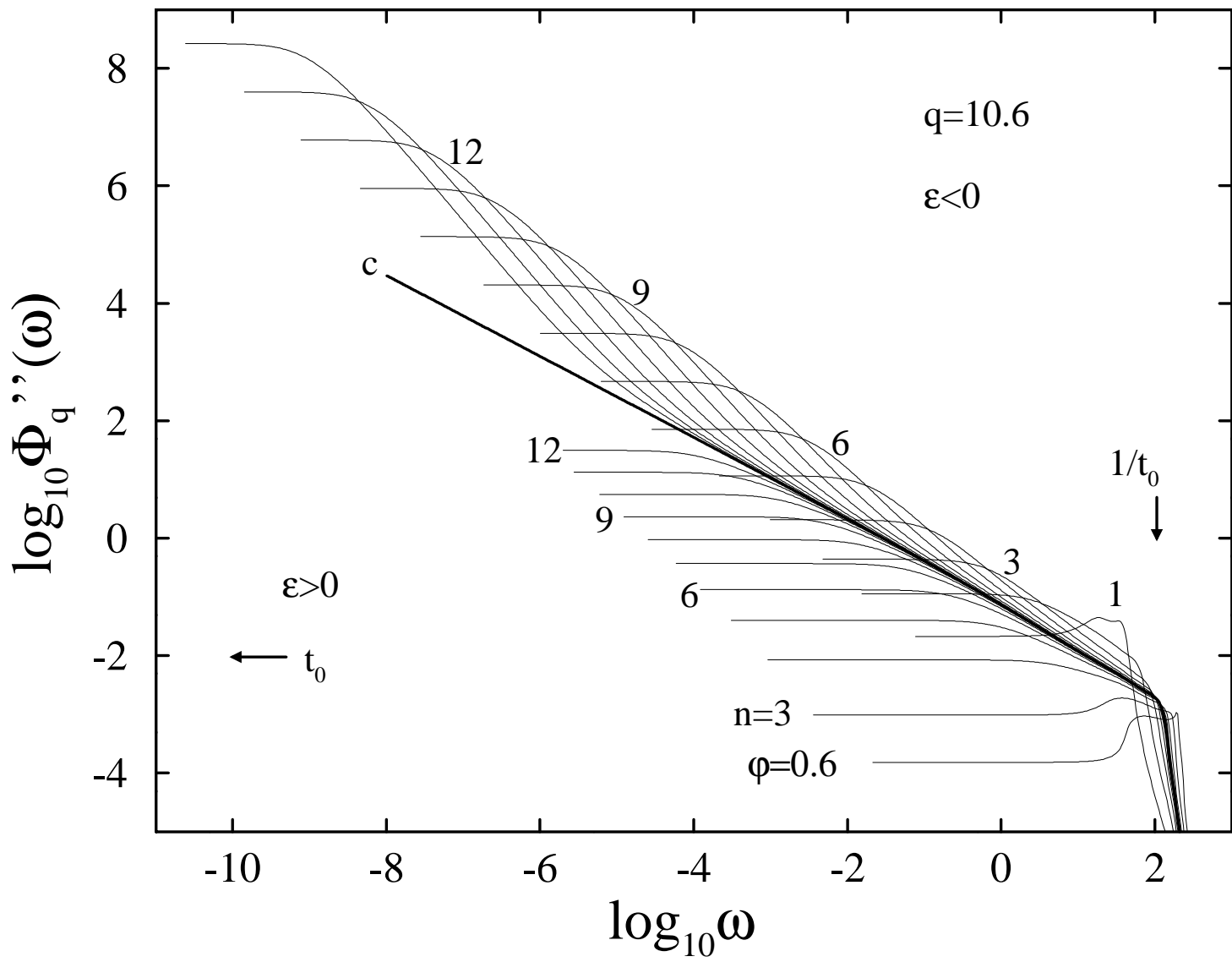
FIG. 15.

Susceptibility spectra for the HSS. The labeling of the curves is done as in Fig. 1. The full lines are calculated for the relaxator transient, Eq. (6b), the dashed lines for the oscillator model (Eq. (6a)), and the dotted results refer to the discrete dynamics model of Sec. V. The scales  $t_0$  are listed in the caption of Fig. 7.

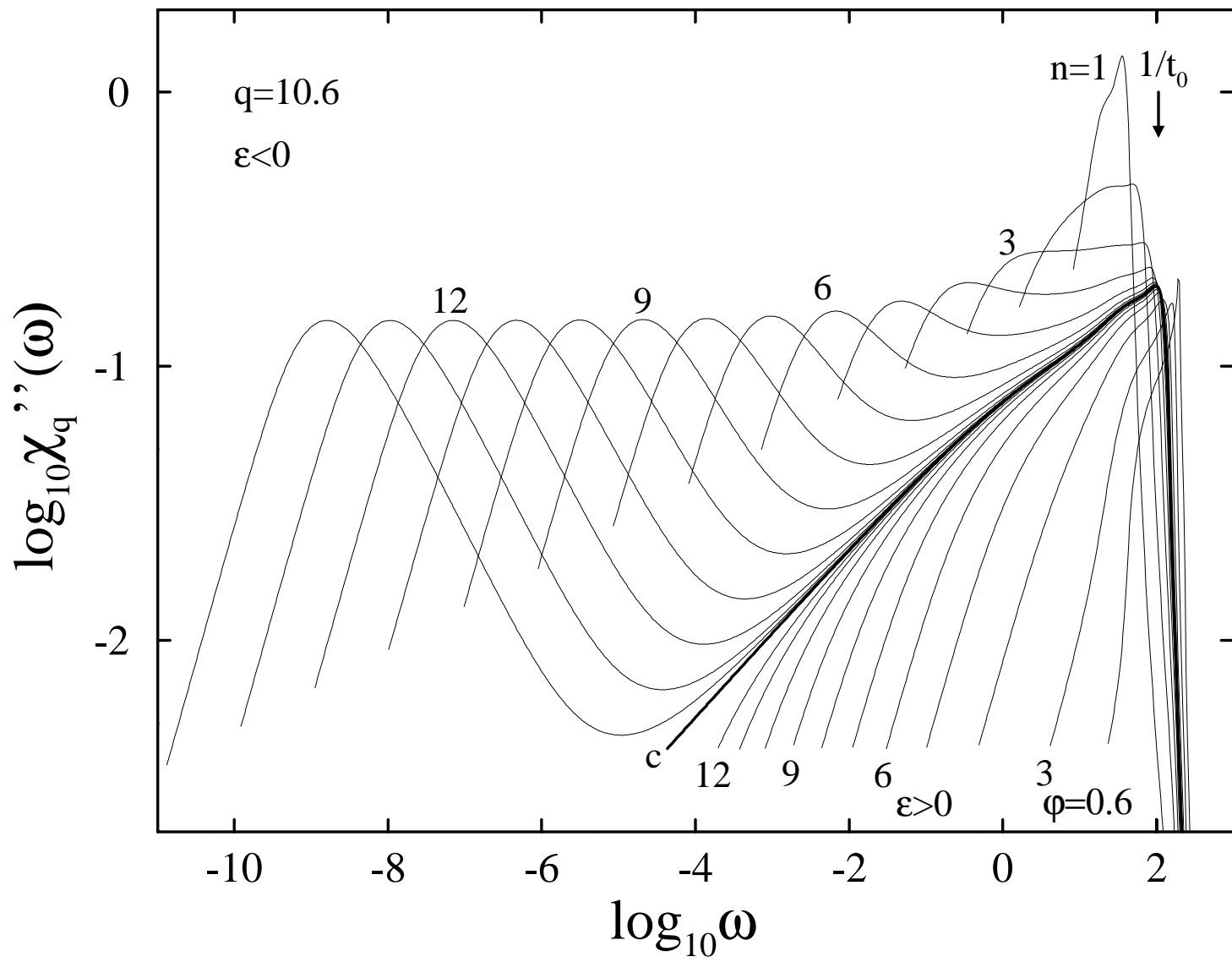
Franosch et al., ... Fig. 1



Franosch et al., ... Fig. 2

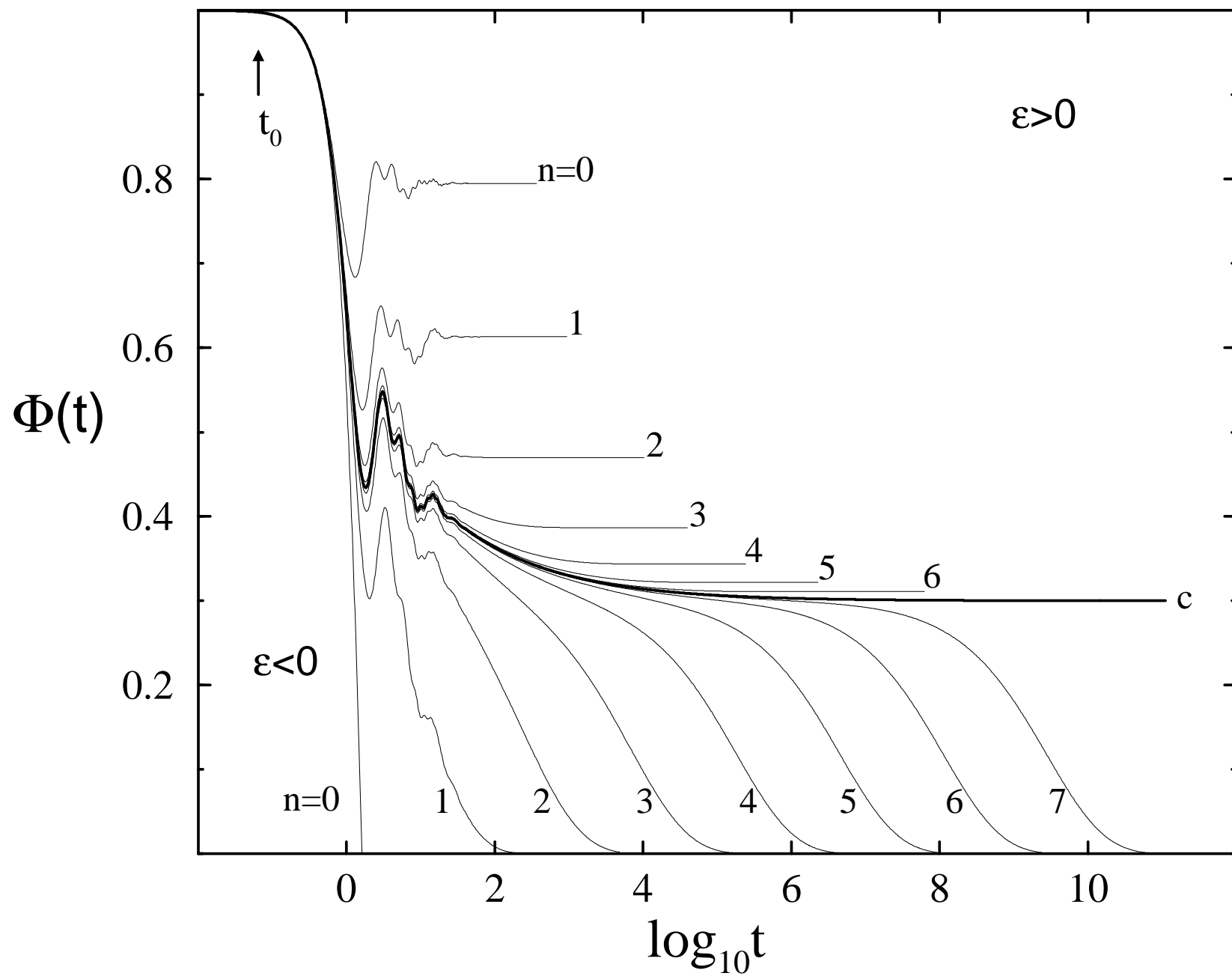


Franosch et al., ... Fig. 3

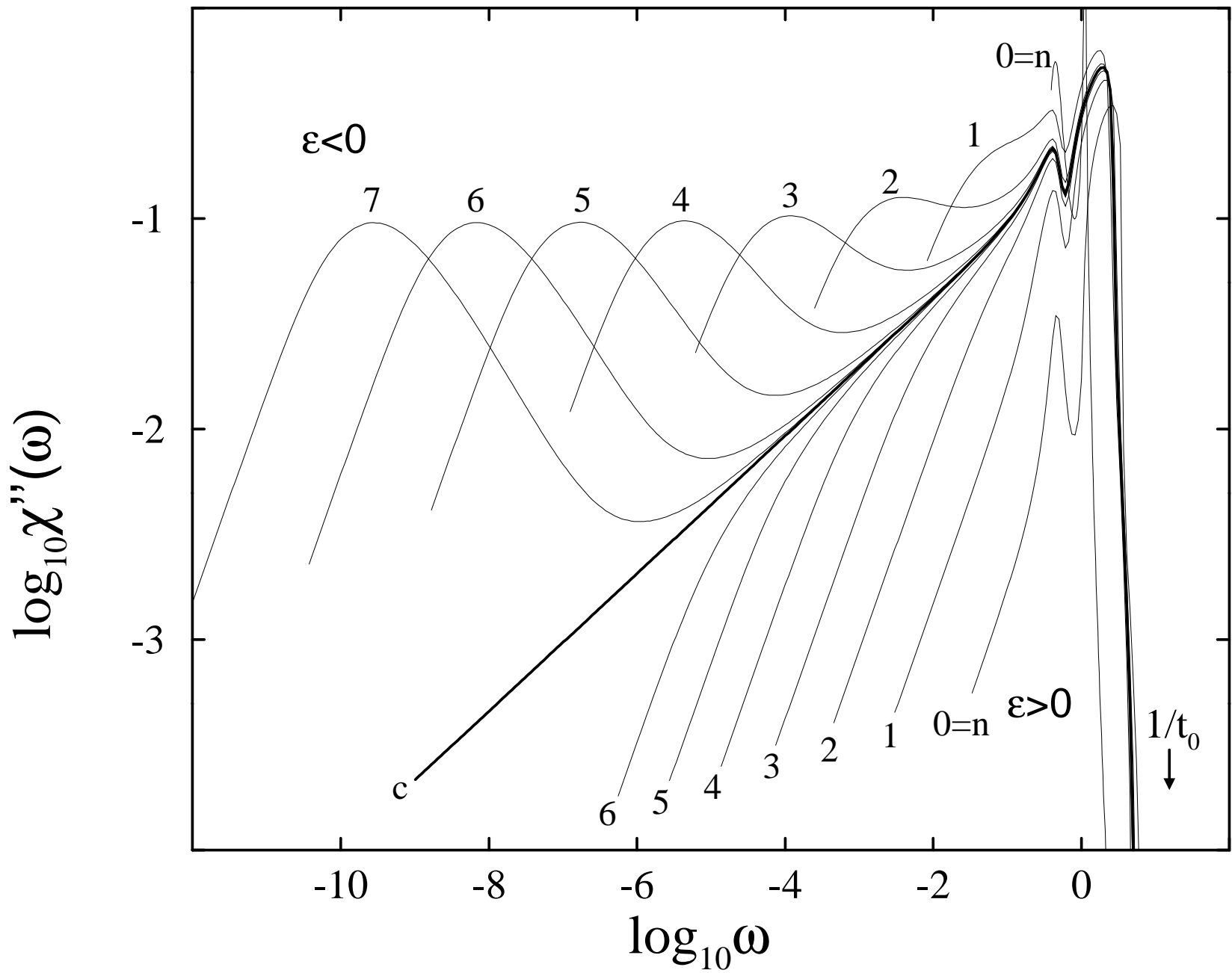




Franosch et al., ... Fig. 4

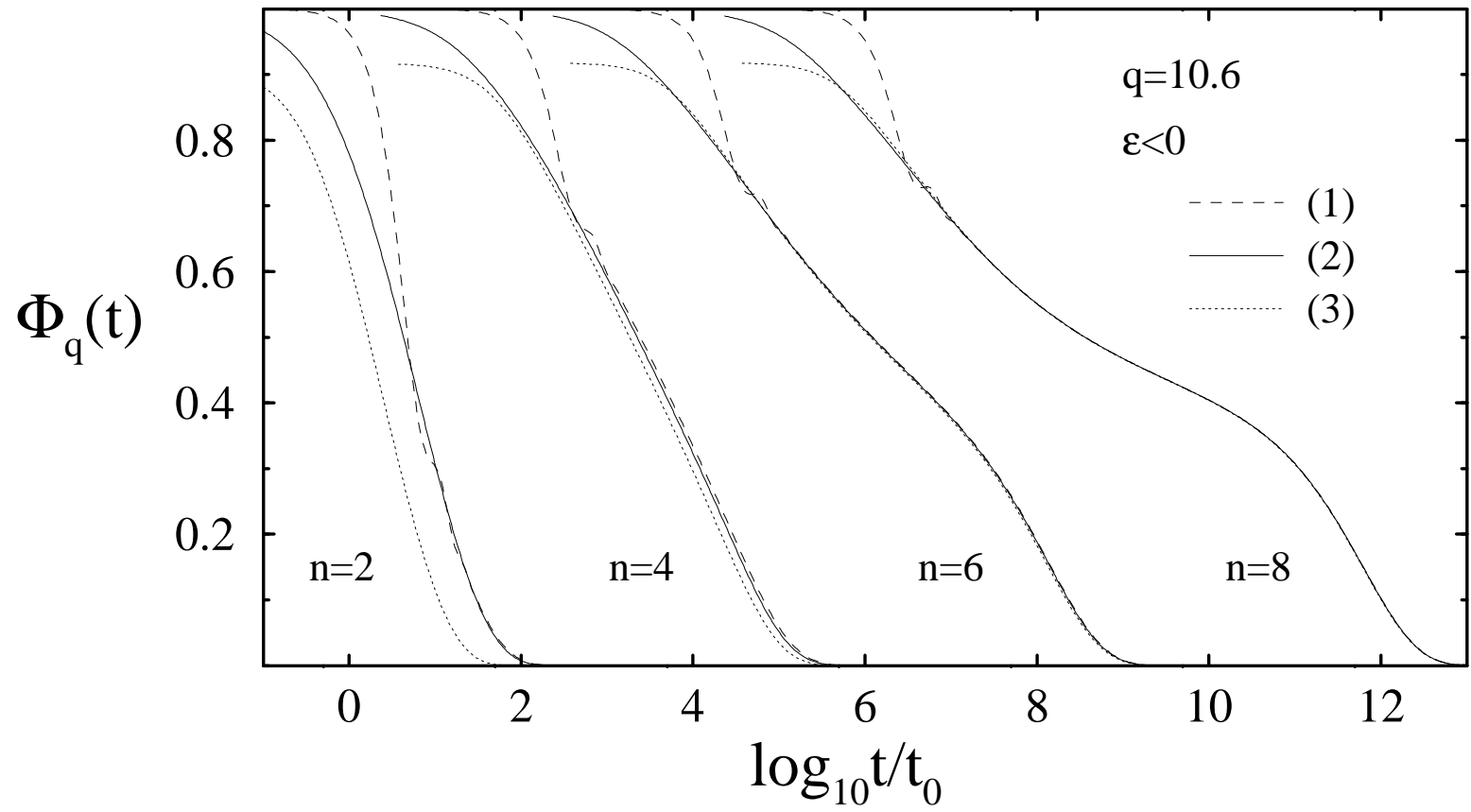


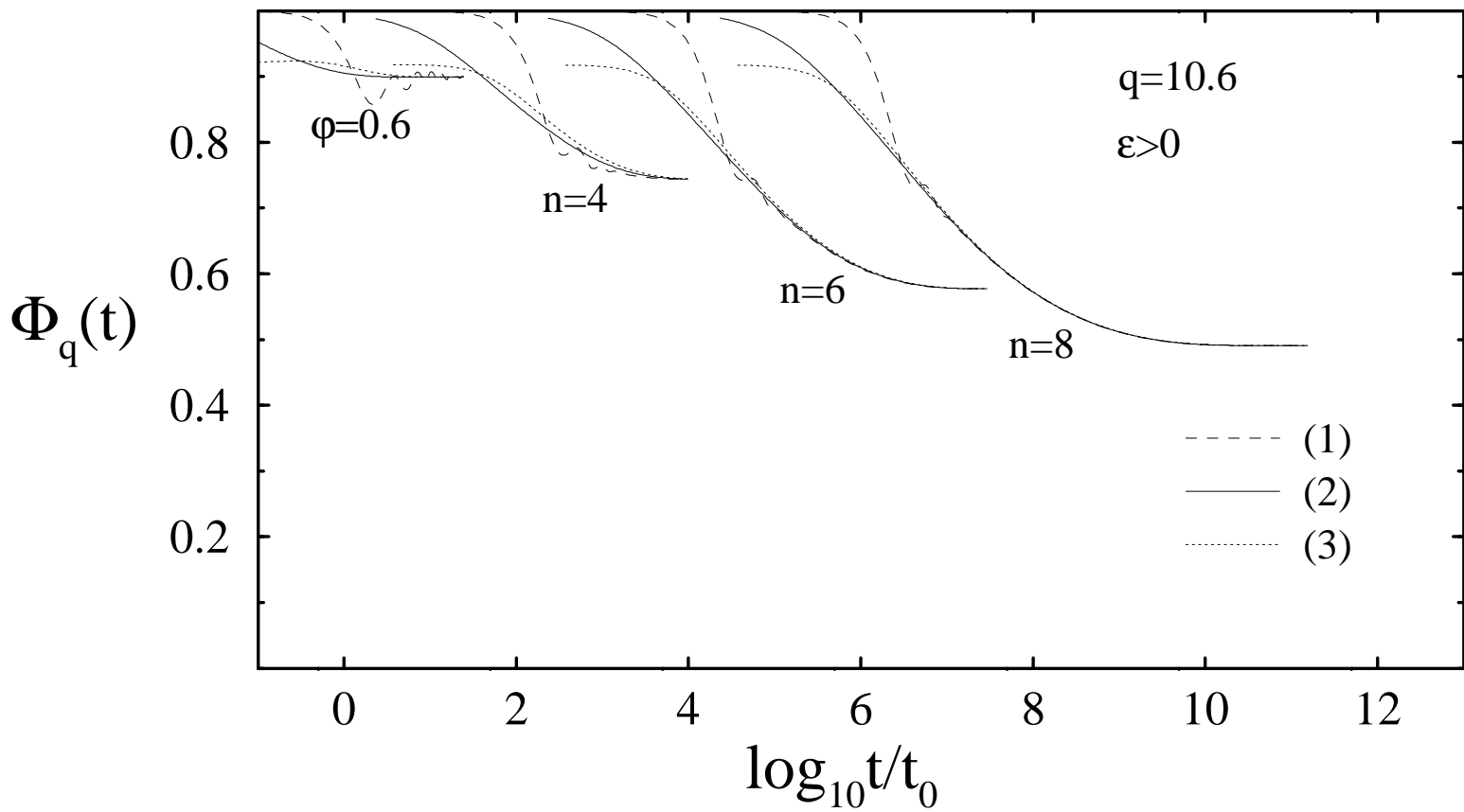




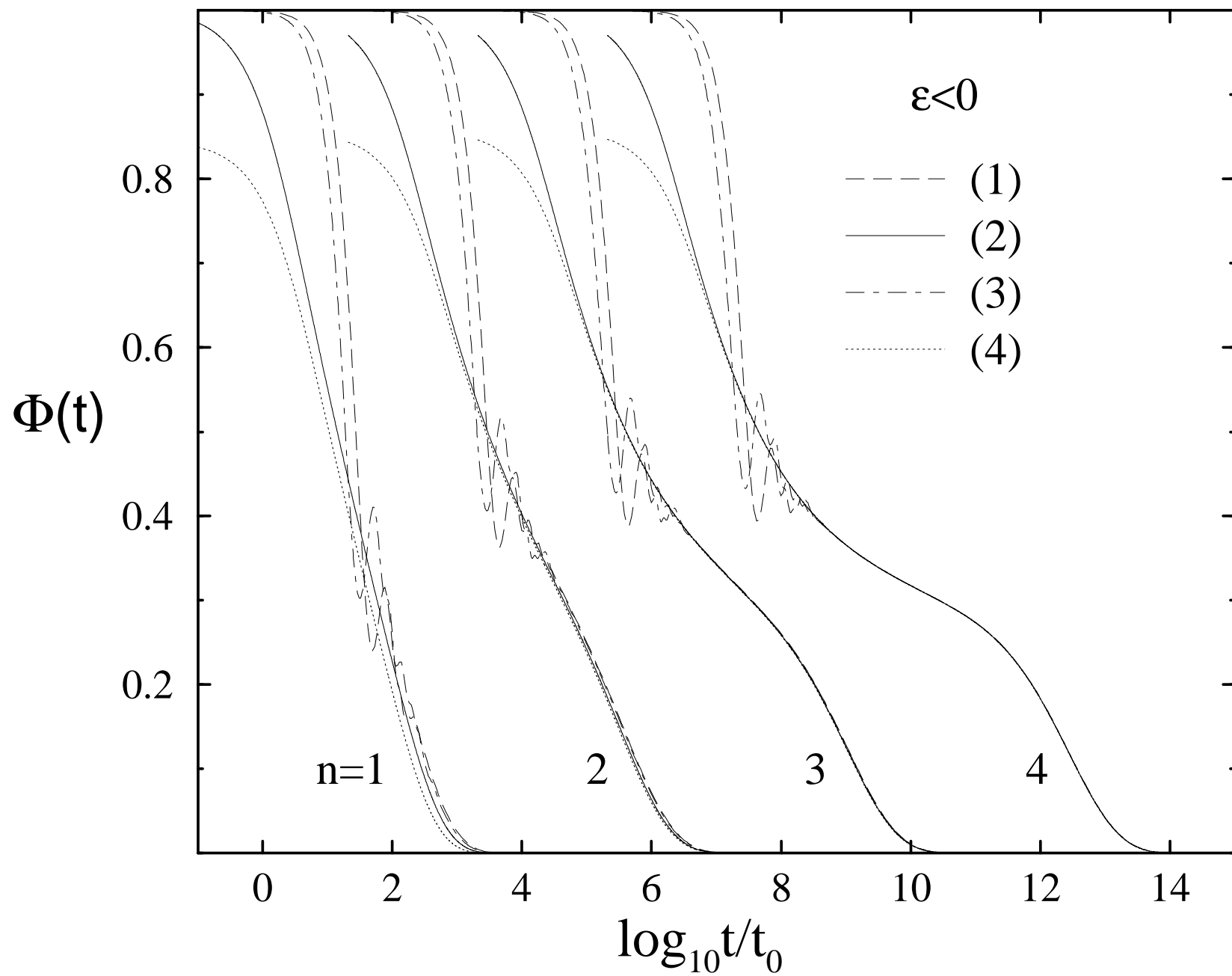
Franosch et al., ... Fig. 6

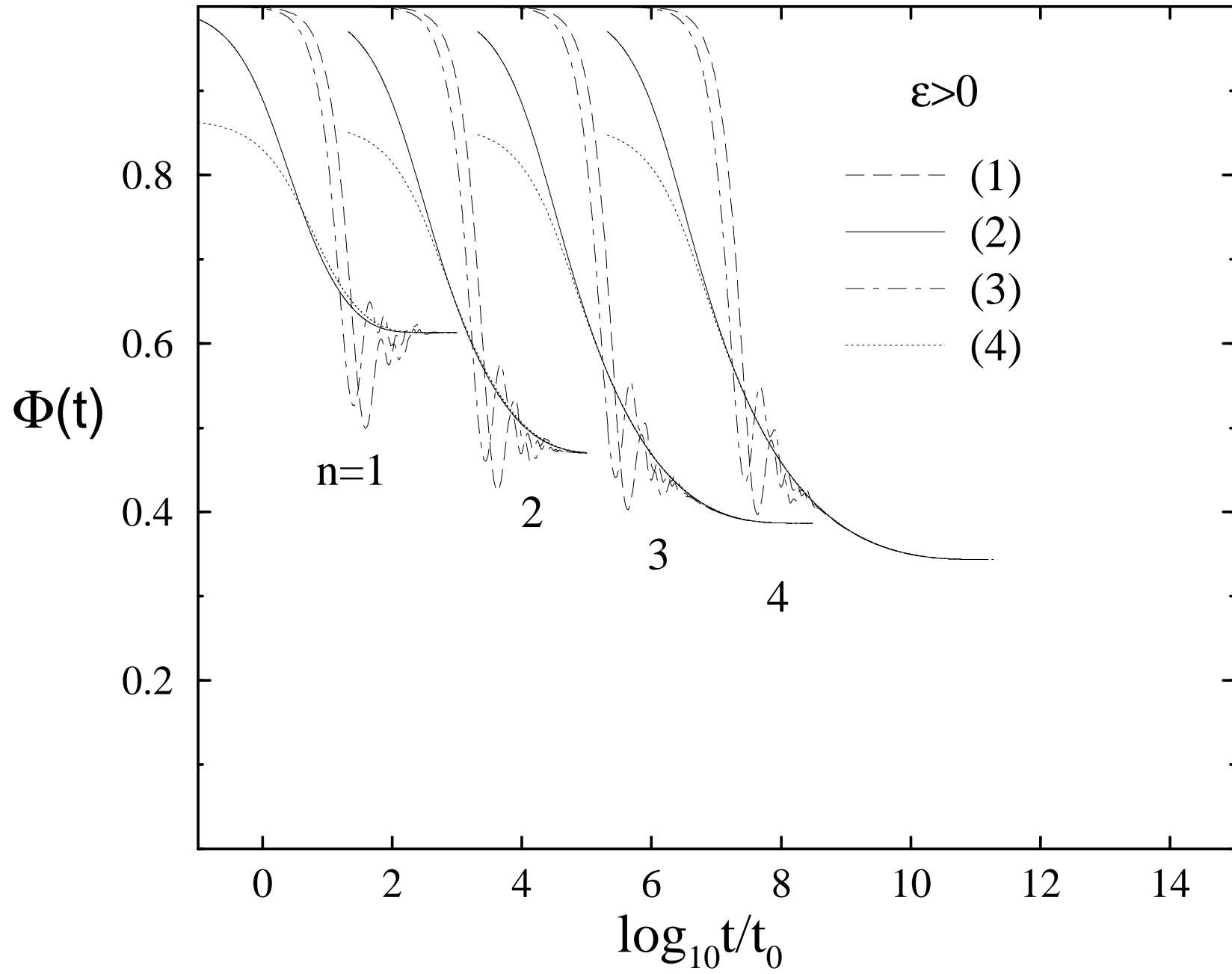
Franosch et al., ... Fig. 7

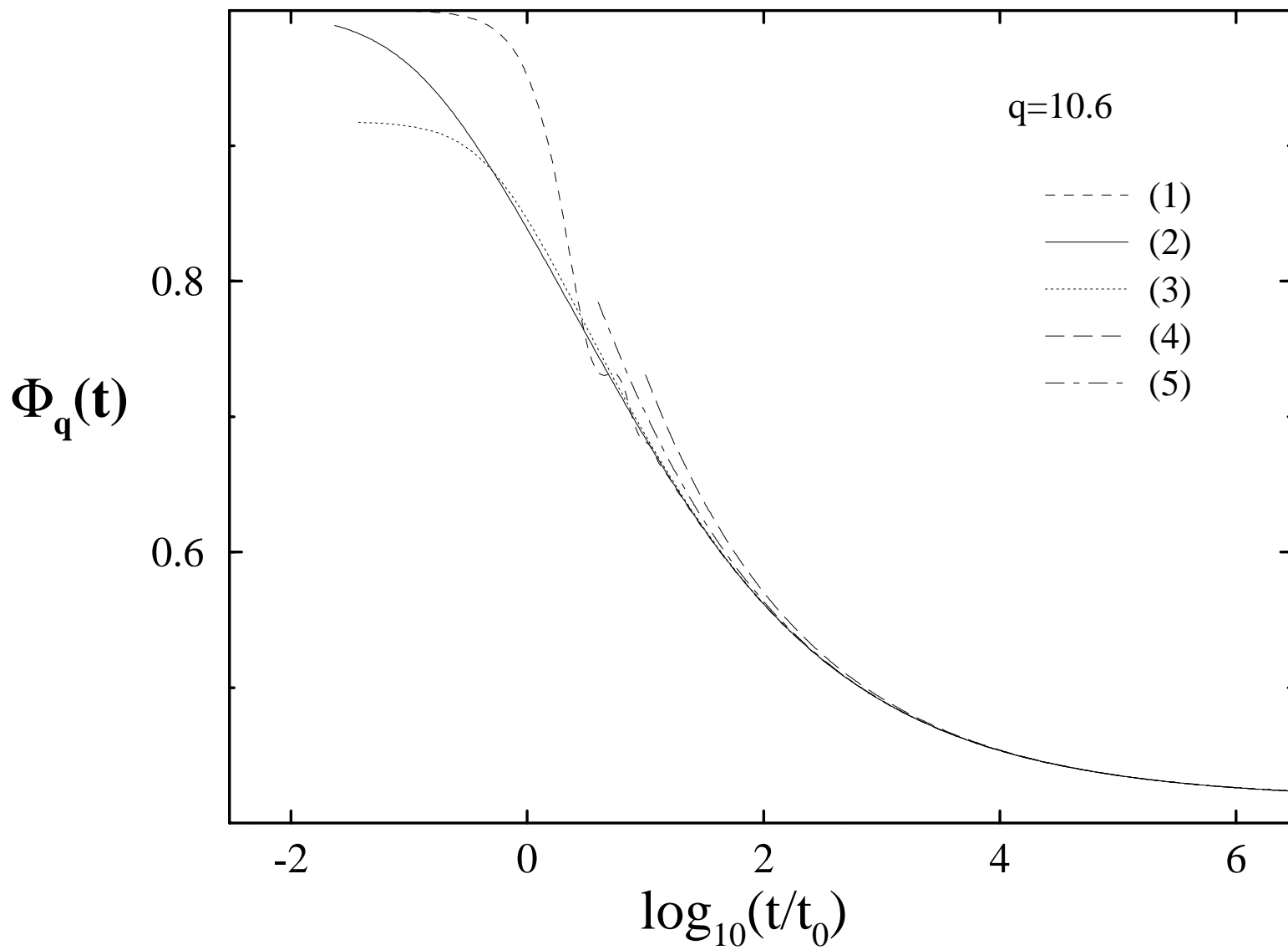




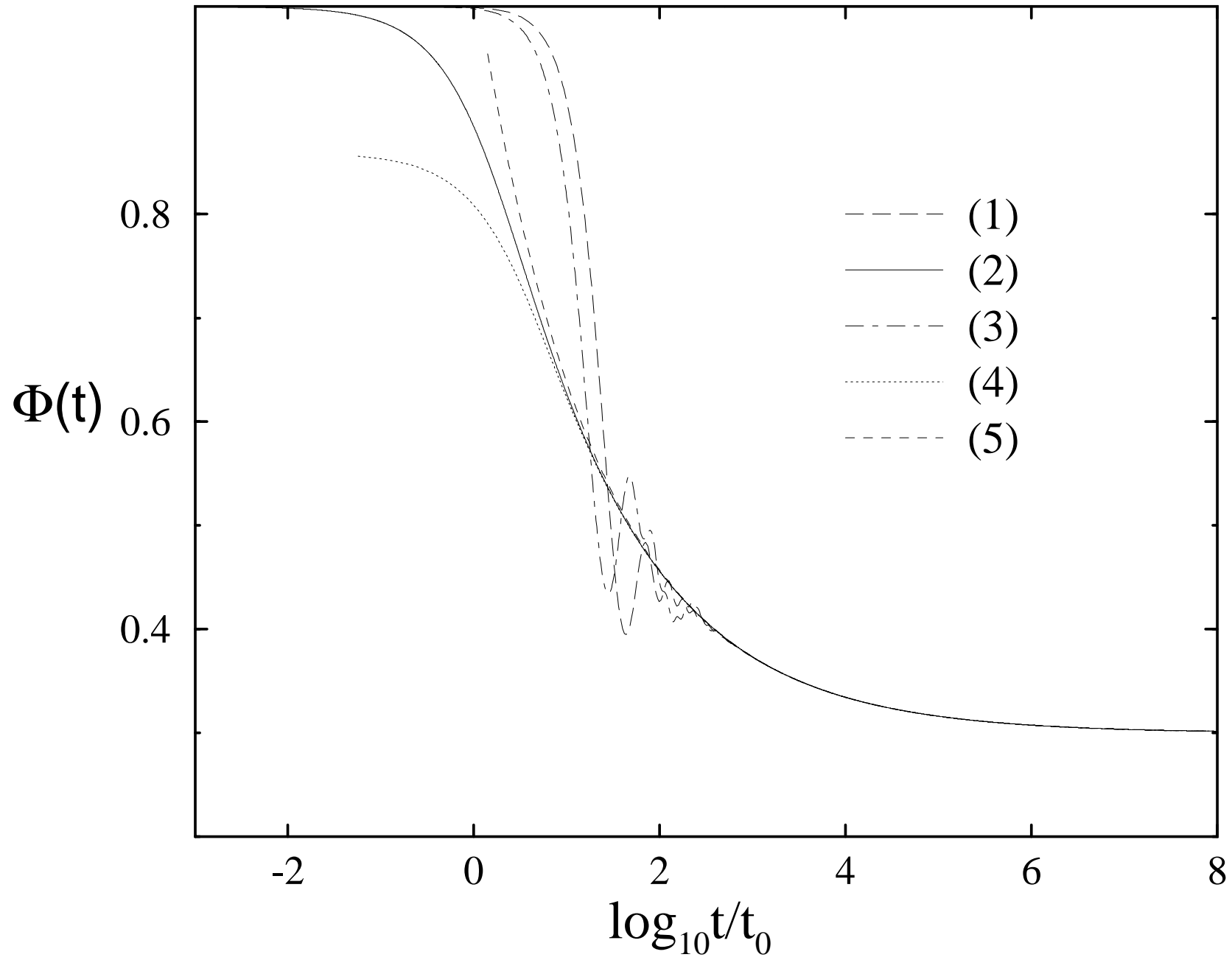
Franosch et al., ... Fig. 9



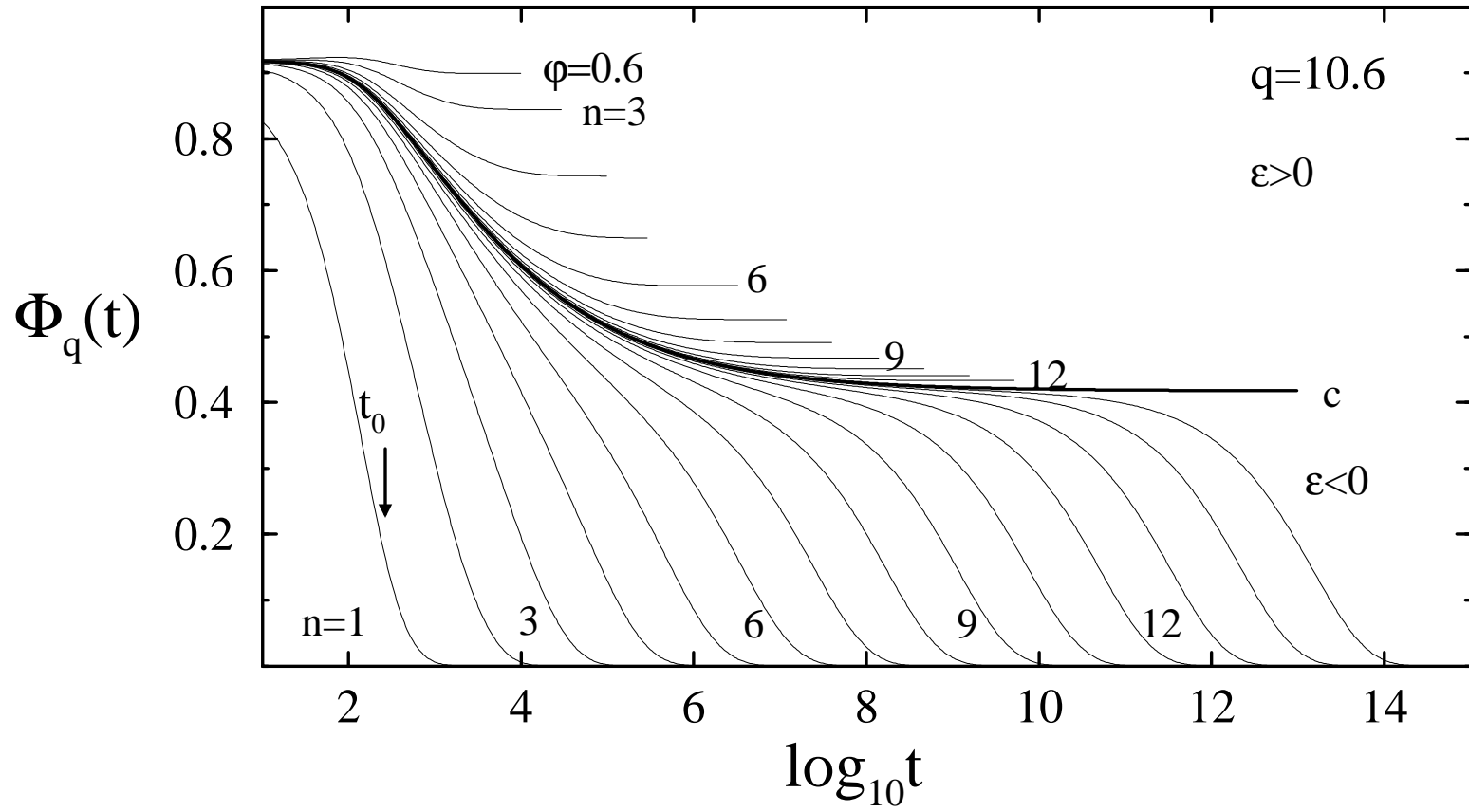




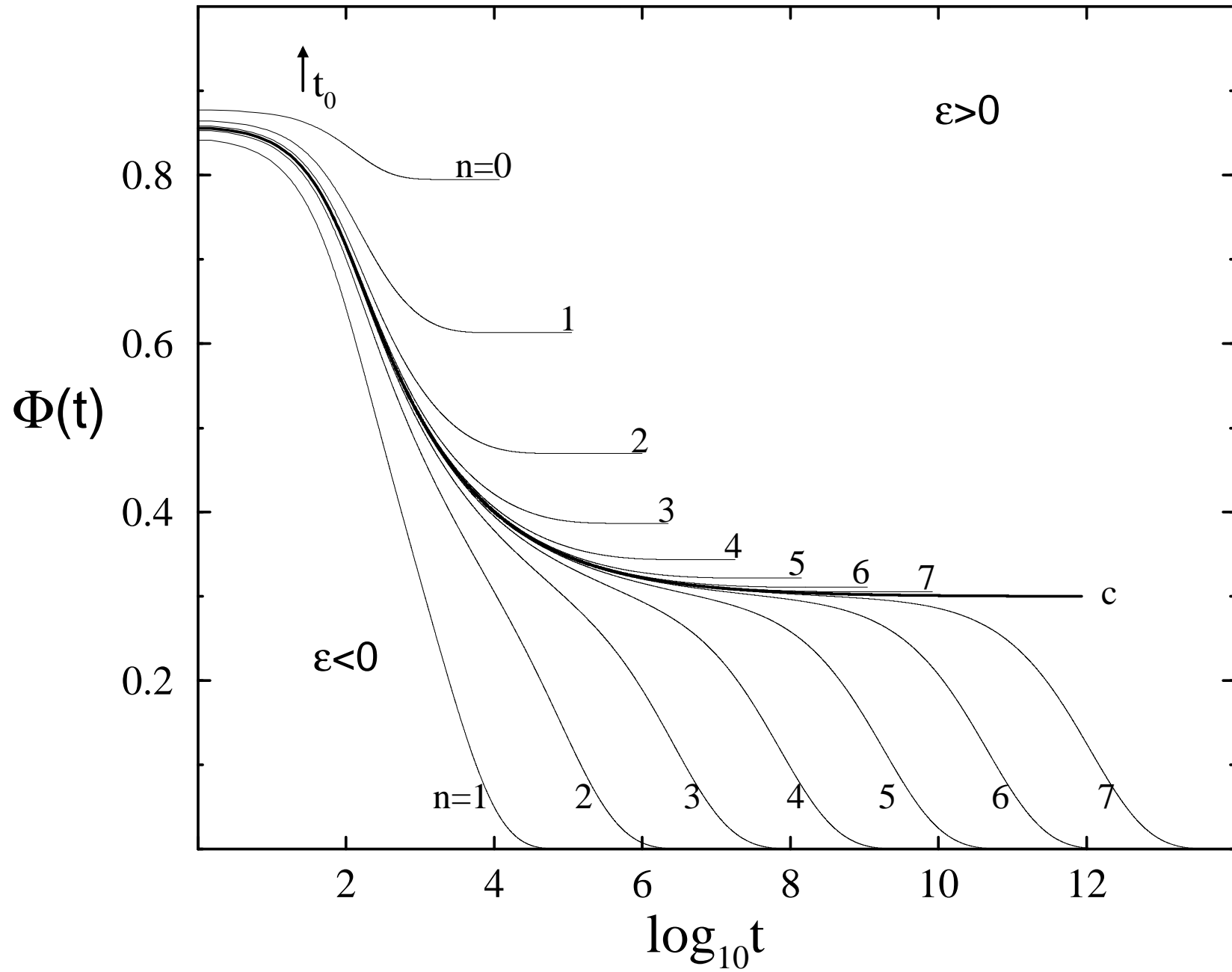




Franosch et al., ... Fig. 13



Franosch et al., ... Fig. 14



Franosch et al., ... Fig. 15

